THE ASTROPHYSICAL JOURNAL, 248:55–60, 1981 August 15

SOFT X-RAY IMAGES OF THE CENTRAL REGION OF THE PERSEUS CLUSTER

G. BRANDUARDI-RAYMONT, D. FABRICANT, E. FEIGELSON, P. GORENSTEIN, J. GRINDLAY, A. SOLTAN,[1] AND G. ZAMORANI[2]
Harvard-Smithsonian Center for Astrophysics, Cambridge, Massachusetts
Received 1980 September 30; accepted 1981 March 2

ABSTRACT

We report the results of 0.5–3.0 keV X-ray observations of the central region of the Perseus cluster carried out with the Imaging Proportional Counter and High Resolution Imager aboard the *Einstein* Observatory. In addition to the very extended thermal cluster emission and a sharply peaked component at NGC 1275 previously known, the high resolution image reveals a point source coincident with the optical nucleus of NGC 1275. The 0.5–3.0 keV luminosity of the compact source is $\sim 10^{44}$ ergs s^{-1}.

The Imaging Proportional Counter data show the cluster emission to be a factor of 1.2 more elongated east-west than north-south. The centroid of the cluster emission is found to be offset 1'.7 east of NGC 1275, in the direction away from the prominent line of galaxies that stretch between NGC 1275 and IC 310. The cluster center determined from galaxy counts lies 6'.4 southwest of the X-ray centroid.

Subject headings: galaxies: clusters of — X-rays: sources

I. INTRODUCTION

Two components of X-ray emission from the Perseus cluster have been identified from a large number of previous observations. The more extended of these (diameter exceeding 1°) is associated with 6–7 keV gas trapped in the potential well of the cluster (Forman *et al.* 1972; Lea *et al.* 1973; Mitchell *et al.* 1976; Serlemitsos *et al.* 1977; Gorenstein *et al.* 1978; Mushotzky 1979; Nulsen and Fabian 1980; Ulmer *et al.* 1980). In addition, an intense and much less extended component (diameter $\lesssim 5'$) surrounding the central galaxy, NGC 1275, was identified (Fabian *et al.* 1974; Helmken *et al.* 1978; Gorenstein *et al.* 1978). It has been suggested that the majority of this emission is produced by cooling gas in the process of accretion onto NGC 1275 (Cowie and Binney 1977; Fabian and Nulsen 1977; Fabian *et al.* 1980). Reports of emission lines characteristic of gas at temperatures near 1 keV from the NGC 1275 region by Canizares *et al.* (1979) and Mushotzky *et al.* (1980) support this view.

None of the X-ray instrumentation prior to the *Einstein* Observatory has had sufficient spatial resolution to unambiguously separate a possible point source from the sharply peaked but extended emission surrounding NGC 1275. In addition, the vastly improved statistical precision of the *Einstein* results allows a more definitive study of the morphology of the extended cluster emission. We describe here observations centered on NGC 1275 made using both of the soft X-ray imaging instruments on board the *Einstein* Observatory. An Imaging Proportional Counter (IPC) observation of 16,500 s effective exposure was begun on 1979 February 2, 23:05 UT. The IPC attains a spatial resolution of ~1'.5 FWHM at 1 keV, over a field of 1°. Its low background, wide field of view, and high efficiency make it preferable for the study of very extended features. A High Resolution Imager (HRI) observation of 12,700 s effective duration followed, beginning on 1979 February 21, 21:58 UT. The HRI and mirror combination attains a resolution of 3″ FWHM on axis and covers a 25′ field of view. Both instruments are described in detail by Giacconi *et al.* (1979).

II. RESULTS

a) IPC Data

The 1° square IPC field of view is filled by the extended cluster emission. Figure 1 (Plate 3) is a 0.5–3.0 keV contour map of the central region of this field superposed on an optical plate of the cluster. The raw data were smoothed by convolution with a Gaussian function of 1'.8 FWHM to minimize spurious statistical fluctuations. The total number of counts is preserved in this process. This map has been corrected for the vignetting effect of the telescope optics. Background counts have not been subtracted, but they account for only 5% of the total at the outermost contour. The contour levels

[1]N. Copernicus Astronomical Center, Warsaw, Poland.
[2]Also, Istituto di Radioastronomia, CNR, Bologna, Italy

are separated by a factor of 1.65 in surface brightness. The two previously known components of X-ray emission are clearly visible in the contour map. At the smoothed IPC resolution of ~2′, the emission is sharply peaked and circularly symmetric around NGC 1275, although noticeable asymmetry at small radii is apparent in the HRI image (Fig. 3). At large radii, where the very extended cluster component dominates, the emission becomes elliptical and its centroid is offset to the east of NGC 1275. Contours beyond the outermost one plotted are not shown because they are distorted by the partial obscuration of the detector window support structure.

To determine the degree of ellipticity, the position angle of the major axis, and the centroid of the cluster emission in a quantitative fashion, the IPC data were binned in 30° segments about a number of trial centers. Only those counts falling between 11′ and 14′ from the trial center were used to avoid distortions due to NGC 1275 and the window support structure. Background determined from long exposure fields containing no strong sources was subtracted, although this is a small correction. The remaining counts were corrected for the vignetting of the telescope and the parameters of the ellipticity found by searching for minimum χ^2.

If the azimuthally averaged surface brightness may be approximated as $S \propto r^{-n}$ in the region of interest, the elliptical dependence may be expressed as

$$S(r,\theta) \propto \left[r\sqrt{1-\varepsilon \cos(\theta-\theta_0)} \right]^{-n}$$

in polar coordinates, where θ_0 is the position angle of the major axis. In this expression, ε is a simple function of the eccentricity e [$\varepsilon = e^2/(2-e^2)$]. Thus, for small ε, the number of counts between two angular limits, θ_1 and θ_2, is:

$$N(\theta_1,\theta_2) \propto \int_{\theta_1}^{\theta_2} \left[1+\frac{\varepsilon n}{2} \cos 2(\theta-\theta_0) \right] d\theta. \quad (1)$$

Integrating,

$$N(\theta_1,\theta_2) \propto 1+\frac{\varepsilon n}{4(\theta_2-\theta_1)} \cos 2(\theta_m-\theta_0) 2 \sin(\theta_2-\theta_1), \quad (2)$$

where

$$\theta_m = \frac{\theta_2+\theta_1}{2}.$$

In the present case, where $n=1.76$ (see Fig. 2) and $\theta_2-\theta_1$ is 0.524 radians (30°),

$$N(\theta_1,\theta_2) \propto 1+0.84\varepsilon \cos 2(\theta_m-\theta_0). \quad (3)$$

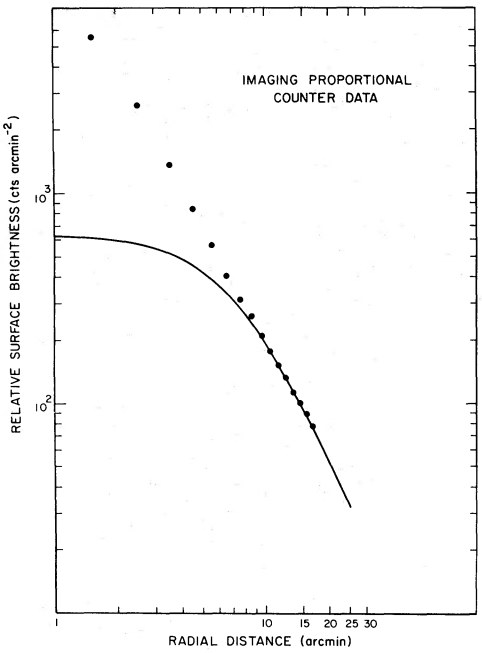

FIG. 2.—The 0.5–3.0 keV azimuthally averaged surface brightness profile of the Perseus cluster centered on NGC 1275. Background from charged particles and the diffuse X-ray background have been subtracted, and a correction for the off-axis vignetting of the X-ray telescope has been made. The solid line is an isothermal hydrostatic fit to the data from 10′ to 17′ ($\beta=0.592$, $a=8'$). The statistical errors are smaller than the plotting symbols.

The centroid of the cluster emission (between 11′ and 14′) is found to be 1.′73±0.′13 east of the X-ray peak coincident with NGC 1275. The allowed parameter ranges determined from fits of equation (3) to the data are $\varepsilon=0.153\pm0.023$ and $\theta_0=92\pm5°$, where θ_0 is measured from north to east. The quoted error limits correspond to the point at which the χ^2 has increased by 4.6 from the minimum value. In the case where statistical errors dominate and the χ^2 minimum is acceptable ($P>10\%$), these would be the 90% confidence limits for two interesting parameters (Avni 1976). However, the minimum χ^2 found for any purely elliptical model is 21 for 9 degrees of freedom. The formal probability of finding a χ^2 this large is ~1.5% for a model accurately describing the data. This must be compared, however, to the minimum χ^2 of 254 for 11 degrees of freedom calculated for spherical symmetry. At any rate, within the radial limits considered, the cluster emission is elongated in the east-west direction, and the ratio of the major to minor axis of the elongation is ~1.17.

Figure 2 is a 0.5–3.0 keV azimuthally averaged surface brightness profile of the IPC data centered on NGC 1275, extending to a radial distance of 17′. Background estimated from other fields has been subtracted and a vignetting correction applied. At 17′, the background level (X-rays and particles) is less than 10% of the total

counts. The data were binned in radial rings about NGC 1275 to minimize the distortions at small radii that would occur if the data were binned about the centroid of the cluster emission. The resulting profile does clearly show the surface brightness peak associated with NGC 1275. However, at the IPC spatial resolution, no compact source can be resolved from the sharply rising background of the extended emission.

If the standard spherically symmetric hydrostatic models for the X-ray–emitting gas trapped in the potential well of the cluster are applied (Lea 1975; Gull and Northover 1975; Cavaliere and Fusco-Femiano 1976; Shibazaki *et al.* 1976; Sarazin and Bahcall 1977), results very similar to those reported by Gorenstein *et al.* (1978) are found. In particular, the same problem reconciling the optical observables (the core radius of the galaxy distribution and the cluster velocity dispersion) and the X-ray observables (the gas temperature and distribution) is encountered. In the case where the galaxies and X-ray–emitting gas are treated as independent, ideal, isothermal gases that respond to the total gravitational mass of the cluster, the density of the gas is related to that of the galaxies by the expression (Cavaliere and Fusco-Femiano 1976):

$$\frac{\rho_{\rm gas}}{\rho_{\rm gas}(0)} = \left[\frac{\rho_{\rm gal}}{\rho_{\rm gal}(0)}\right]^{\beta}, \qquad (4)$$

where

$$\beta \equiv \frac{\mu M_{\rm H} \sigma_v^2}{kT_{\rm gas}}$$

(μ is the mean molecular weight of the gas particles; σ_v is the line-of-sight velocity dispersion of the galaxies; $M_{\rm H}$ is the hydrogen atom mass; $T_{\rm gas}$ is the X-ray gas temperature).

When β is calculated using $\sigma_v = 1307 \pm \sim 150$ km s^{-1} (Tifft 1978), $\mu = 0.6$ (Allen 1973), and $kT = 6.4 \pm 0.4$ (Mushotzky 1979), the value 1.65 ± 0.39 is found. Using the observed galaxy distribution in the central region of the cluster, $\rho_{\rm gal}(r) \propto [1+(r/a)^2]^{-3/2}$, (Bahcall 1974) and equation (4), the X-ray surface brightness should be given by:

$$S \propto \left[1+(r/a)^2\right]^{-3\beta+1/2}$$

(r measured in arc minutes; a, the core radius of the galaxy distribution, is 8′). On the other hand, when models of this type are fitted to the data in the range 10′–17′ (avoiding NGC 1275) leaving β free and fixing the core radius at 8′, β is required to be 0.592 ± 0.015 (at 90% confidence). This is a factor of 2–3 smaller than the β calculated using the observed σ_v. Explanations for this discrepancy may involve a large deviation from spherical symmetry or a misleading estimate of one of the optical observables, the core radius, or velocity dispersion. These questions may possibly be addressed with X-ray data taken at large distances from the cluster center.

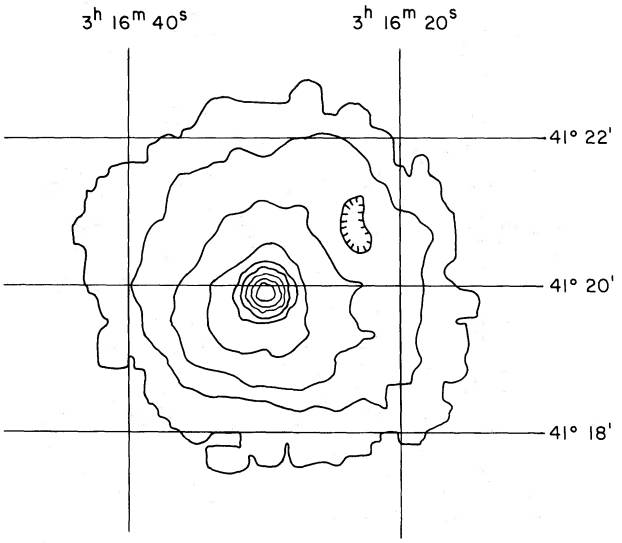

FIG. 3.—A contour plot of the HRI data. The data have been smoothed with a 16″ (FWHM) Gaussian weighting function. The contour levels are separated by a factor of 1.6 in surface brightness. The contour to the NW with tick marks is at the same level as the next outer large contour.

At any rate, we have used the $a = 8'$, $\beta = 0.59$ model to estimate the contribution of the NGC 1275 region above what might be expected from the cluster source alone. We find that 40% of the IPC counts within a projected radius of 25′ (the cluster fit is extrapolated from 17′ to 25′) are in excess of those predicted by the model for the cluster emission.[3] A total of 20.2 IPC cts s^{-1} are detected in the 0.5–3.0 keV band within a projected radius of 17′; extrapolated to 25′ this becomes 23.3 cts s^{-1}.

b) HRI Data

Figure 3 is an HRI contour map of a region 2′ in radius centered on NGC 1275. Instrumental background has not been subtracted, but fewer than 10% of the counts at the outermost contour are background. The contour levels are separated by a factor of 1.6 in surface brightness. The map has been smoothed by convolution with a Gaussian function of 16″ FWHM to minimize the effect of statistical fluctuations. The total number of counts are preserved in the smoothing process. The

[3]Comparison of this figure with that reported by Gorenstein *et al.* 1978 (25%) revealed an error in the earlier paper. The 25% actually referred to the normalization of an assumed Gaussian model with a 2.5 FWHM. When this model is integrated to give the total number of counts due to NGC 1275, a figure of ~38% is calculated, in agreement with the present result.

emission is not azimuthally symmetric on scales less than 1′, but is considerably more symmetric on larger scales, consistent with the IPC image. Fabian *et al.* (1980) relate the HRI image to optical features of NGC 1275. A point source is located at $\alpha(1950)=3^h16^m29^s.7$ $\delta(1950)=40°19'54''$ to an accuracy of $\sim 5''$. This is consistent with both the optical location of NGC 1275's nucleus and the position of the radio source 3C 84 (Wade and Johnston 1977; Cohen 1972).

Figure 4 is the azimuthally averaged surface brightness profile produced with the HRI data from a region 8′ in radius, centered on NGC 1275. The plotted data have been corrected for the vignetting of the telescope optics, and the instrumental background has been subtracted. In addition to the data, the response of the HRI and X-ray mirror combination to a point source of 1.5 keV X-rays and the cluster emission model ($a=8'$, $\beta=0.59$) discussed in connection with the IPC data are shown. The HRI profile was normalized to the IPC surface brightness profile in the region 3′–8′ (the radial dependences are very similar) and the cluster emission model transferred to the HRI assuming that the ratio of NGC 1275 to cluster counts is the same in the two instruments. Figure 5 is an azimuthally averaged plot of the HRI data with the contribution of the point source subtracted. The dashed curve in Figure 5 is given by $0.567/[1+(r/74)^2]$ cts arcsec^{-2} (r measured in arc seconds) which is a good description of the data beyond 40″.

During the HRI observation of 12,700 s, 43,900 counts were detected within a projected radius of 9′. Of these, 5000 are due to the point source. The normalization of this component has been determined by fitting an analytic description of the instrumental point source response plus a power law of variable slope to the data within 1′. When the counts originating at radii (spherical coordinates) beyond 9′ (estimated from the surface brightness at 9′) and those due to the point source are subtracted, 29,200 counts remain.

III. DISCUSSION AND CONCLUSIONS

The high resolution image of NGC 1275 provides the first unambiguous observation of a compact X-ray source coincident with the optical nucleus of NGC 1275. The HRI count rate of 0.39 cts s^{-1} observed from the compact source may be converted into a flux or normalization if a spectral shape and intrinsic absorption are assumed. Primini *et al.* (1980) have recently reported that the spectrum of the Perseus cluster contains a hard component in addition to the previously known 6.4 keV thermal spectrum at energies above 15 keV. The excess is fitted by a spectrum of the form $dN/dE=5\times 10^{-2}E^{-1.9}$ photons cm^{-2} s^{-1} keV^{-1}. They suggest that the excess might either be due to a compact source or an inverse Compton process (involving the scattering of relativistic particles off the 3 K background) taking place at much larger scales within the cluster.

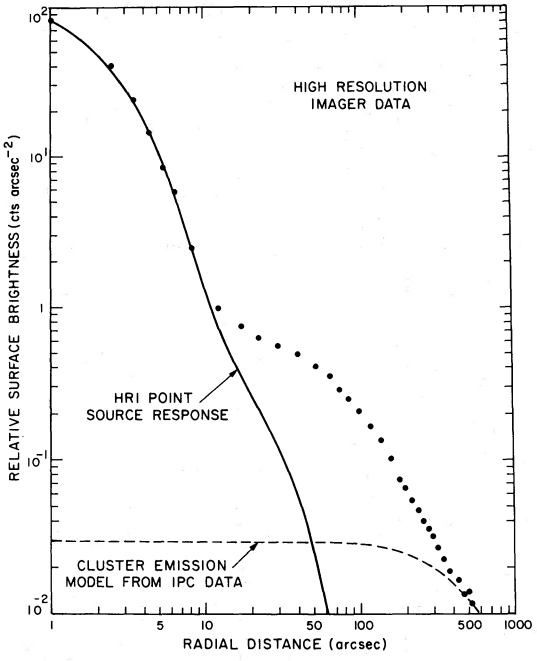

FIG. 4

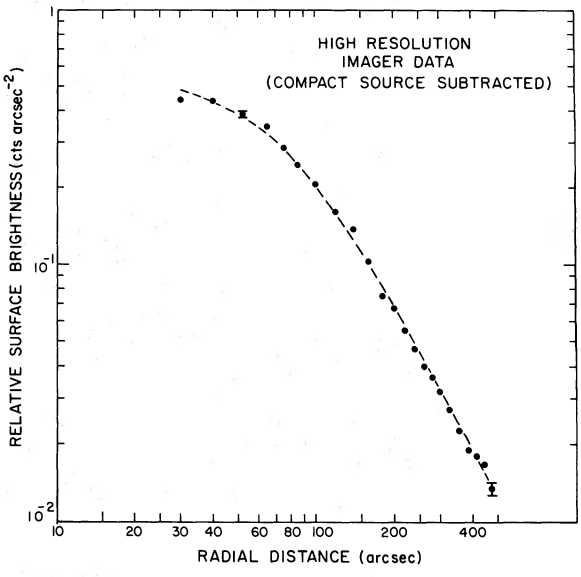

FIG. 5

FIG. 4.—The HRI azimuthally averaged surface brightness profile centered on NGC 1275. Background has been subtracted, and a correction for the off-axis vignetting of the X-ray telescope has been made. The statistical errors are smaller than the plotting symbols.

FIG. 5.—The same data plotted in Fig. 4, but the contribution of the compact source has been subtracted. The dashed line is given by $0.567/[1+(r/74'')^2]$ cts arcsec^{-2}.

TABLE 1

PHOTON SPECTRUM NORMALIZATION DERIVED FROM HRI COUNT RATE OF NUCLEUS OF NGC 1275

INTRINSIC ABSORPTION EXPRESSED AS N_H	PHOTON SPECTRAL INDEX ASSUMED	
	1.9	1.5
0	1.9×10^{-2}	1.9×10^{-2}
4.3×10^{21}	4.8×10^{-2}	4.1×10^{-2}
8.6×10^{21}	7.1×10^{-2}	5.7×10^{-2}
13.0×10^{21}	9.2×10^{-2}	7.0×10^{-2}

Table 1 lists the normalization derived from the HRI count rate and the known spectral sensitivity for spectra of the form $dN/dE \propto E^{-1.9}$ and $dN/dE \propto E^{-1.5}$ with various values of intrinsic absorption (expressed as equivalent hydrogen column densities). The column density in our Galaxy has been taken to be 1.6×10^{21} atoms cm^{-2} (Gorenstein *et al.* 1978). A spectrum of the form $dN/dE \propto E^{-1.5}$ has been included since this is typical of that observed from a wide variety of active galactic nuclei. Gorenstein *et al.* (1978) derive an expected absorbing column equivalent to 4.3×10^{21} atoms cm^{-2} from measurements of reddening in the nucleus of NGC 1275. If this intrinsic absorption is coupled with a photon spectrum of index 1.9, the normalization is found to be 4.8×10^{-2} photons cm^{-2} s^{-1}, essentially identical to the value given by Primini *et al.* (1980). The agreement suggests the identification of the hard spectral component with the nuclear source. The 0.5–3.0 keV luminosity of the point source is $1.2\pm0.4\times10^{44}$ ergs s^{-1} ($H_0=50$ km s^{-1} Mpc^{-1}) for the eight spectra considered in Table 1. This is in the range found for Seyfert type 1 galaxies (Kriss, Canizares, and Ricker 1980). The calculated luminosity is a factor of 2 lower if the spectrum of the compact source is assumed to be the same as that of the cluster (thermal, with $kT\sim6.5$ keV).

The HRI image has also allowed the determination of the 0.5–3.0 keV surface brightness profile of the extended emission surrounding NGC 1275 to high accuracy. A remaining impediment to the use of the X-ray data to describe the physical conditions near NGC 1275 is the uncertain temperature distribution in the X-ray–emitting gas, which cannot be determined directly with the HRI. However, Fabian *et al.* (1980) have used a modified constant pressure deconvolution technique to estimate the temperature and density profiles of this gas. They derive a temperature distribution that decreases radially inward, with the temperature at 1′ a factor $\gtrsim2$ lower than that at 8′. The HRI count rate of 2.3 cts s^{-1} from the central region of 9′ radius (point source subtracted) corresponds to 0.5–3.0 keV luminosities in the range $3–5\times10^{44}$ ergs s^{-1}, as the assumed mean gas temperature is allowed to vary between 6.5 and 1.0 keV. The region surrounding NGC 1275 is over an order of magnitude more luminous than the equivalent region surrounding M87, another galaxy with well-studied extended thermal emission (Fabricant, Lecar, and Gorenstein 1980). The observed IPC count rate of 23.3 cts s^{-1} extrapolated to a projected radius of 25′ corresponds to a 0.5–3.0 keV luminosity of $1.12\pm0.05\times10^{45}$ ergs s^{-1}. The quoted error includes the effect of varying the assumed gas temperature between 1.0 and 6.5 keV. As before, the column density has been taken to be 1.6×10^{21} cm^{-2}. The luminosities of various regions in the cluster are summarized in Table 2. We assume throughout that $H_0=50$ km s^{-1} mpc^{-1} and adopt a redshift of 0.0182 (Chincarini and Rood 1971).

Under the assumptions of spherical symmetry, hydrostatic equilibrium, and an isothermal gas, the observed IPC surface brightness profile and luminosity may be used to calculate the total mass of X-ray–emitting gas and the total gravitational mass within a given radius. Because the assumption of isothermality is unlikely to be valid for radii less than 10′, these quantities have only been calculated in the region beyond 10′. For a gas temperature of 6.4 keV, $\sim1.9\times10^{13}$ $M_\odot$ of gas are necessary to produce the observed luminosity between radii of 10′ and 17′. If the observed surface brightness profile is extrapolated to 25′, this number increases to 4.6×10^{13} $M_\odot$ for the 10′–25′ region. Fabian *et al.* (1980) estimate that 10^{13} $M_\odot$ of gas are contained within a radius of 10′, leading to a total of $\sim5.8\times10^{13}$ $M_\odot$ of gas within 25′ of NGC 1275. Equation (7) of Fabricant, Lecar, and Gorenstein (1980) may be used to estimate the total gravitational mass:

$$-\frac{kT_{\rm gas}}{G\mu M_{\rm H}}\left(\frac{d\log\rho_{\rm gas}}{d\log r}\right)r=M_*(r) \qquad (5)$$

($T_{\rm gas}$ = gas temperature; $\rho_{\rm gas}$ = gas density; μ = mean molecular weight (taken to be 0.6); G = gravitational constant; $M_{\rm H}$ = mass of hydrogen atom; $M_*(r)$ = total mass within radius r).

TABLE 2

0.5–3.0 keV LUMINOSITIES OF VARIOUS REGIONS WITHIN THE PERSEUS CLUSTER ($H_0=50$ km s^{-1} Mpc^{-1})

Region	Luminosity
Point source at NGC 1275	$1.2\pm0.4\times10^{44}$ ergs s^{-1}
Region of 9′ radius surrounding NGC 1275 (point source subtracted)	$4\pm1\times10^{44}$ ergs s^{-1}
Region of 25′ radius surrounding NGC 1275	$1.12\pm0.05\times10^{45}$ ergs s^{-1}

For $T_{gas}=6.4$ keV, $r=17'$ (or 1.65×10^{24} cm), and $d\log\rho_{gas}/d\log r=1.46$, the total mass within 17′ is found to be $1.9\times10^{14}\ M_\odot$. If the modeled surface brightness is extrapolated to 25′, this number rises to $3.0\times10^{14}\ M_\odot$.

If one accepts the description of the galaxy distribution as that of a self-gravitating isothermal sphere (Bahcall 1974), one may calculate the dynamical mass within any given radius based on the velocity dispersion of the galaxies and the core radius of the isothermal sphere (here taken to be 8′). This mass is proportional to the square of the line-of-sight velocity dispersion if the velocity dispersion is isotropic. One finds by this method a dynamical mass of $\sim9\times10^{14}\ M_\odot$ within a radius of 25′, a factor of 3 higher than that calculated from the X-ray data. This is consistent with the disagreement mentioned previously between the β calculated using the measured velocity dispersion ($\beta\propto\sigma_v^2$, also) and that determined from the X-ray surface brightness profile and the 8′ core radius of the galaxies.

The ellipticity of the cluster X-ray surface brightness contours indicates that the cluster potential well is somewhat flattened. The comparison of the X-ray data with the galaxy counts as reported by Bahcall (1974) is not straightforward because she does not explicitly discuss the optical isodensity contours. Bahcall finds that the width at half-maximum of the galaxy surface density averaged over strips 45′ long, is 8.′4 for the strips that are parallel to the line of galaxies, and 16.′8 for the strips that are perpendicular. This is the often quoted 2:1 optical anisotropy of the Perseus cluster. The significance of this ratio is not obvious because the presence of the bright line of galaxies greatly enhances the counts in the central strip parallel to it. If one attempts to estimate (from Bahcall's Fig. 2) the relative widths at equal galaxy surface density at radii of 15′ to 20′, a ratio more like 1.2 or 1.3 is found, consistent with the X-ray data. However, the optical center of the cluster reported by Bahcall, $\alpha(1950)=3^h16^m.1$, $\delta(1950)=41°18'.5$, is not coincident with the X-ray centroid at $\alpha=3^h16^m.65$, $\delta=41°19'.9$, within the estimated optical measurement error of 3′. Because the X-ray–emitting gas is pervasive and responds to all the mass in the cluster regardless of whether it is optically luminous or not, X-ray observations probably now provide the most reliable means of determining the distribution of that mass.

The authors acknowledge useful discussions with A. Cavaliere, G. Chincarini, A. Fabian, R. Mushotzky, and F. Primini. G. Zamorani acknowledges support from a European Space Agency fellowship.

REFERENCES

Allen, C. W. 1973, *Astrophysical Quantities* (London: Althone).
Avni, Y. 1976, *Ap. J.*, **210**, 642.
Bahcall, N. 1974, *Ap. J.*, **187**, 439.
Canizares, C., Clark, G., Markert, T., Berg, C., Smedira, M., Bardas, D., Schnopper, H., and Kalata, K. 1979, *Ap. J.* (*Letters*), **234**, L33.
Cavaliere, A., and Fusco-Femiano, R. 1976. *Astr. Ap.*, **49**, 137.
Chincarini, G., and Rood, H. 1971, *Ap. J.*, **168**, 321.
Cohen, M. 1972, *Ap. Letters*, **12**, 81.
Cowie, L., and Binney, T. 1977, *Ap. J.*, **215**, 723.
Fabian, A., Hu, E., Cowie, L., and Grindlay, J. 1980, *Ap. J.*, submitted.
Fabian, A., and Nulsen, P. 1977, *M.N.R.A.S.*, **80**, 479.
Fabian, A., Zarnecki, J., Culhane, J., and Hawkins, F. 1974, *Ap. J.* (*Letters*), **189**, L59.
Fabricant, D., Lecar, M., and Gorenstein, P. 1980, *Ap. J.*, **241**, 552.
Forman, W., Kellogg, E., Gursky, H., Tananbaum, H., and Giacconi, R. 1972, *Ap. J.*, **178**, 308.
Giacconi, R., *et al.* 1979, *Ap. J.*, **230**, 540.
Gorenstein, P., Fabricant, D., Topka, K., Harnden, F. R., Jr., and Tucker, W. 1978, *Ap. J.*, **224**, 718.
Gull, S., and Northover, K. 1975, *M.N.R.A.S.*, **173**, 585.
Helmken, H., Delvaille, J., Epstein, A., Geller, M., Schnopper, H., and Jernigan, J. 1978, *Ap. J.* (*Letters*), **221**, L43.
Kriss, G., Canizares, C., and Ricker, G. 1980, *Ap. J.*, **242**, 492.
Lampton, M., Margon, B., and Bowyer, S. 1976, *Ap. J.*, **208**, 177.
Lea, S. 1975, *Ap. Letters*, **16**, 141.
Lea, S., Silk, J., Kellogg, E., and Murray, S. 1973, *Ap. J.* (*Letters*), **184**, L105.
Mitchell, R., Culhane, J., Davison, P., and Ives, J. 1976, *M.N.R.A.S.*, **176**, 29P.
Mushotzky, R. 1979, Erice Symposium on X-Ray Astronomy.
Mushotzky, R., Holt, S., Smith, B., Boldt, E., and Serlemitsos, P. 1980, *Ap. J.*, in press.
Nulsen, P., and Fabian, A. 1980, *M.N.R.A.S.*, **191**, 887.
Primini, F., Basinska, E., Howe, S., Lang, F., Levine, A., Lewin, W., Rothschild, R., Baity, W., Gruber, B., Matteson, J., Peterson, L., Lea, S., Reichert, G. 1980, *Ap. J.* (*Letters*), **243**, L13.
Sarazin, C., and Bahcall, J. 1977, *Ap. J. Suppl.*, **34**, 451.
Serlemitsos, P., Smith, B., Boldt, E., Holt, S., and Swank, J. 1977, *Ap. J.* (*Letters*), **221**, L63.
Shibazaki, N., Hoshi, R., Takahara, F., and Ikenchi, S. 1976, *Prog. Theor. Phys.*, **56**, 1475.
Tifft, W. 1978, *Ap. J.*, **222**, 421.
Ulmer, M., *et al.* 1980, *Ap. J.*, **236**, 58.
Wade, C., and Johnston, K. 1977, *A.J.*, **82**, 791.

G. BRANDUARDI-RAYMONT: Mullard Space Science Laboratory, Holmbury St. Mary, Dorking, Surrey, England

D. FABRICANT, E. FEIGELSON, P. GORENSTEIN, J. GRINDLAY, and G. ZAMORANI: Harvard-Smithsonian Center for Astrophysics, 60 Garden Street, Cambridge, MA 02138

A. SOLTAN: N. Copernicus Astronomical Center, Bartycka 18, 00-716 Warsaw, Poland

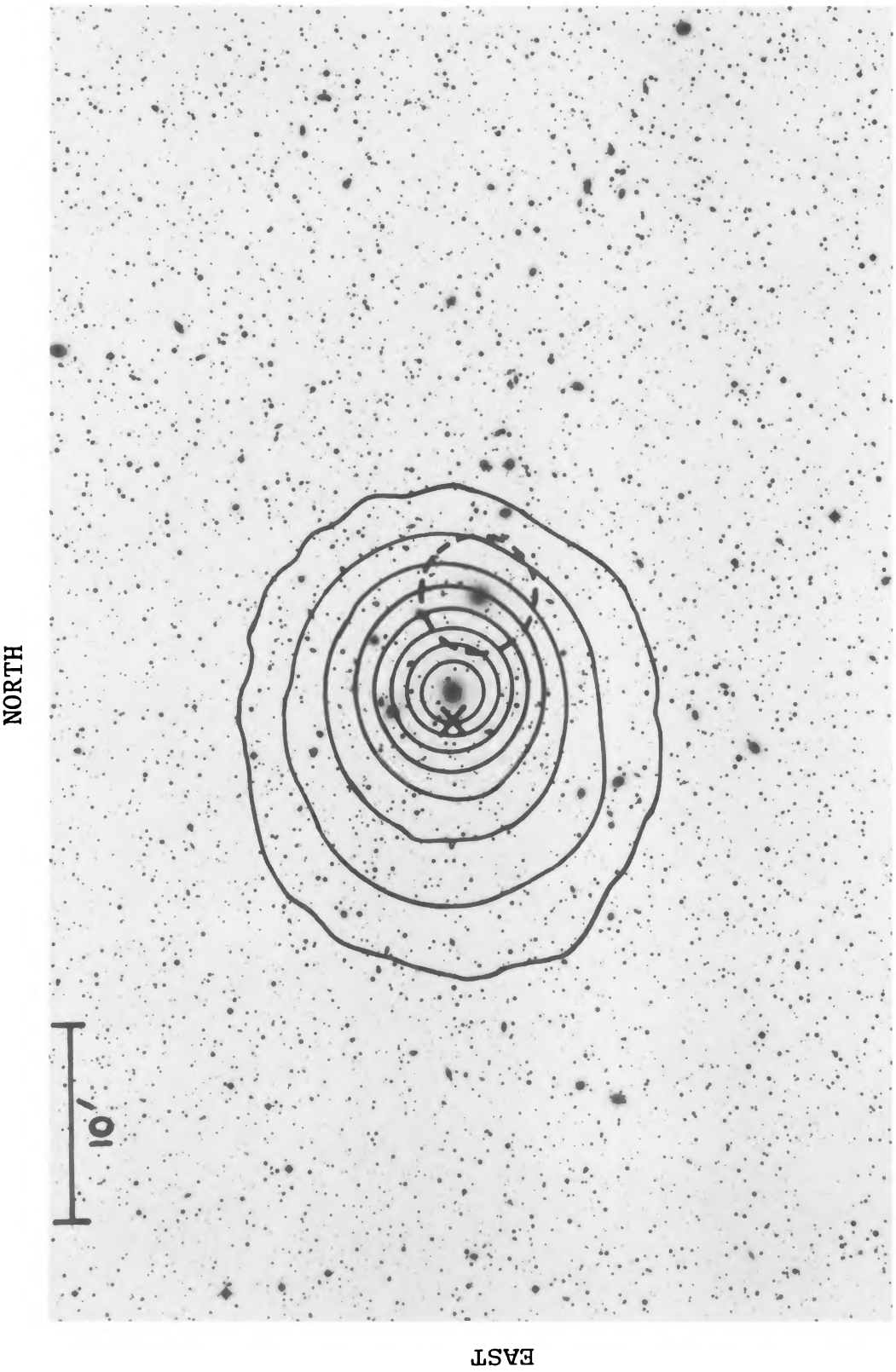

FIG. 1.—A 0.5–3.0 keV contour plot of the IPC corrected data superposed on an optical plate of the central region of the Perseus cluster. The data have been smoothed with a 1′.8 (FWHM) Gaussian weighting function and corrected for the off-axis vignetting of the X-ray telescope. The contour levels are separated by a factor of 1.65 in surface brightness. The dashed circle is the optical cluster center (Bahcall 1974), and the X marks the centroid of the X-ray emission. Only the contours within 17′ of NGC 1275 are displayed. A larger field is shown in the optical photograph for reference.